One pot synthesis of low cost emitters with large Stokes' shift

One pot synthesis of low cost emitters with large Stokes' shift

G. Volpi,[a] G. Magnano,[a] I. Benesperi, [a] D. Saccone, [a] E. Priola, [a,c] V. Gianotti, [b] M. Milanesio,[b,c] E. Conterosito,[b] C. Barolo,[* a,d] G. Viscardi[a]

[a] *Dipartimento di Chimica, NIS Interdepartmental Centre and INSTM Reference Centre , Università di Torino, Via Pietro Giuria 7, 10125, Torino, Italy. Fax: +39 011 670 7591; Tel: +39 011 670 7596; E-mail: claudia.barolo@unito.it*

[b] *Università del Piemonte Orientale Dipartimento di Scienze e Innovazione Tecnologica Viale T. Michel 11, I-15121 Alessandria, Italy*

[c] *CrisDi Interdepartmental Center for Crystallography*

[d] *ICxT Interdepartmental Centre*

* corresponding author

Keywords: imidazo[1,5-*a*]pyridine, fluorescence, large Stokes' shift, quantum yield, down-shifting.

Abstract

A series of 1,3-diarylated imidazo[1,5-*a*]pyridine derivatives were synthesized in high yields by a one-pot, three components, condensation of phenyl(pyridin-2-yl)methanone with several aldehydes in the presence of ammonium acetate. These compounds were characterized by spectroscopic and crystallographic techniques and their optical properties were discussed in relation to their chemical structures. Absorption and fluorescence spectra generally show two absorption maxima around 310 nm and 350 nm and an emission maximum between 460-550 nm with a remarkable Stokes' shift range of 90-166 nm. Moreover, depending on the chemical structure of the substituent in position 3, we were able to tune the quantum yields (Φ) in solution from 6.4% to 38.5%. Finally, the 1-phenylimidazo[1,5-*a*]pyridine substituted with a 3-(2-

methoxyphenyl) group (large Stokes' shift, high Φ) was dispersed in a transparent thermosetting polyurethane resin giving a luminescent low cost material.

1. Introduction

Large Stokes' shift organic emitting molecules are acquiring a great interest due to their potential application as low-cost and eco-friendly active compounds in down-shifting luminescent layers both in lighting [1] and photovoltaic (PV) technologies [2]. Moreover, luminescent solar concentrators (LSC) based on thin-film organic molecules represent a convenient technology to improve power conversion efficiency of PV systems [3].

Two of the most important prerequisites for a good candidate molecule for down-shifting and LSC applications are a large Stokes' shift (to avoid re-absorption) and a high quantum yield [4]. It is of paramount importance that absorbed photons are re-emitted and not dissipated as heat. In previous studies regarding down-shifting technologies, the choice of fluorophores has been focused on molecules with a very high quantum yield (95%), but a very small Stokes' shift [5]. While the high quantum yield ensures that almost every absorbed photon is then re-emitted, the very small Stokes' shift leads to a very high re-absorption. In these conditions, a photon may be re-absorbed several times before it can reach the working layer of the photoelectric device. Since the emission of the molecule is isotropic and not focused, a high photon loss is unavoidable. In this work we focused our attention on imidazo[1,5-*a*]pyridine derivatives, a class of UV absorbers that is well known for biological activities [6-11], but which also shows unique photophysical properties. These compounds have been applied in a large variety of fields, including organic thin-layer field effect transistors (OFETs) [12] and organic light-emitting diodes (OLEDs) [13]. This class of compounds is known for its large Stokes' shift, but these

dyes generally show too low quantum yields for practical applications [14-15]. A deep synthetic effort, in conjunction with a solid photophysical and structural characterization [16], is therefore needed in order to understand which are the moieties able to improve the emission behavior without decreasing the Stokes' shift properties. For this purpose, we synthesized and characterized eleven 3-substituted-1-phenylimidazo[1,5-*a*]pyridines (Figure 1). Concerning the synthetic approach, several methods have been recently reported involving the use of Pd-catalyzed [14] and Cu-catalyzed reactions on different substrates [17]. Less recently, most reactions were conducted starting from amines and ketones or aldehydes either in the presence of a sensitive Lewis acid [18] or of a stoichiometric amount of elemental sulphur (S_8) as an oxidant [15], or from the oxidation of a Schiff base [19]. Unfortunately, all these methods require two or three steps from the initial reagents [20] and careful processing due to the use of highly sensitive reagents, thus hampering an easy scale up of the synthesis towards industrial application. Nonetheless, an efficient synthetic method for the preparation of the imidazo[1,5-*a*]pyridine moiety has also been proposed via a three component condensation reaction using pyridylketones, aldehydes and ammonium acetate [21]. In the present work, we selected this last synthetic approach, due to its simplicity and low cost of reagents, with promising scale up perspectives. This method allowed us to introduce different substituents, enhancing the conjugation length and introducing electron-donating or electron-withdrawing moieties in position 3 of the 1-phenylimidazo[1,5-*a*]pyridine skeleton. In compounds **3** and **10** an OH group in the ortho position of the substituent was inserted in order to verify the possibility for the molecules to undergo an Excited State Intramolecular Proton Transfer (ESIPT) [22] fluorescence mechanism. In compound **8** a triphenylamine group was added, which is known to be a thermally stable electron-donating group [23] and a charge-transporting species used in nonlinear optics

[24], two-photon absorption [25] and OLED materials [26]. This structural diversity should also imply photofunctional differences making the 1-phenylimidazo[1,5-*a*]pyridines an interesting series of easily tunable photofunctional materials.

Finally, the most promising compound **4** (Figure 1) was also dispersed in a thermosetting polyurethane resin, and its photophysical properties were investigated in the solid state.

Figure 1.

2. Experimental details

2.1 Materials and techniques

All solvents and raw materials were used as received from commercial suppliers (Sigma-Aldrich and Alfa Aesar) without further purification. The two precursors of the polyurethane resin used for the down-shifting tests, a polyol with product name LCR 540RT–DH and an isocyanate with product name DK 100LV, were acquired from S.E. Special Engines Srl. TLC was performed on Fluka silica gel TLC-PET foils GF 254, particle size 25 nm, medium pore diameter 60 Å. Column chromatography was performed on Sigma-Aldrich silica gel 60 (70-230 mesh ASTM). ^{1}H and ^{13}C NMR spectra were recorded on a Bruker Avance 200 spectrometer at 200 MHz and 50 MHz, respectively, in $CDCl_3$ or CD_3OD. Mass spectra were recorded on a Thermo-Finnigan Advantage Max Ion Trap Spectrometer equipped with an electrospray ion source (ESI) in positive or negative ion acquiring mode for **1**, **2**, **6** and **9**. High-resolution mass spectra were recorded on an LTQ Orbitrap Hybrid Mass Spectrometer for compounds **3**-**5**, **7**, **8**, **10** and **11**.

2.2 **Procedure for the preparation of compounds 1-11**

Four compounds of this series (**1**, **2**, **6** and **9**) were previously reported with different synthetic approaches based on the use of a metal catalyst, a Lewis acid or a strong oxidant, as reported in Table 1. Very recently [17b, 17c] also compound **4** has been reported.

Table 1.

2.2.1 *General synthetic procedure*

A mixture of phenyl(pyridin-2-yl)methanone (800 mg, 4.37 mmol, 1 eq), aldehyde (6.55 mmol, 1.5 eq), and ammonium acetate (1704 mg, 21.85 mmol, 5 eq) in glacial acetic acid (25 mL) was stirred at 110 °C under inert atmosphere. After 5 h, the reaction mixture was cooled to room temperature and the acetic acid was removed by evaporation under reduced pressure. The obtained solid was dissolved in a saturated aqueous solution of Na_2CO_3 and the mixture extracted with CH_2Cl_2. The organic layer was separated, dried and the solvent evaporated under vacuum. The obtained crude product was purified via column chromatography on silica gel (CH_2Cl_2-CH_3OH 98:2).

3-methyl-1-phenylimidazo[1,5-*a*]pyridine (**1**)

712 mg, yield = 78.2%

^{1}H NMR (200 MHz, $CDCl_3$): δ 2.50 (s, 3H), 6.36 (t, *J* = 6.6 Hz, 1H), 6.54 (dd, *J* = 6.4 Hz, 9 Hz, 1H), 7.13-7.44 (m, 5H), 7.60 (d, *J* = 9.2 Hz, 1H), 7.79 (d, *J* = 7.4 Hz, 1H)

^{13}C NMR (50 MHz, $CDCl_3$): δ 12.06, 112.18, 118.34, 118.50, 120.70, 125.79, 125.97, 126.02, 128.40, 129.25, 134.56, 134.84

MS (ESI): m/z 209.17$[M+1]^+$

1,3-diphenylimidazo[1,5-*a*]pyridine (**2**) [17]

956 mg, yield = 81.1%; solid, m.p.:120°C

^{1}H NMR (200 MHz, $CDCl_3$): δ 6.54 (ddd, *J* = 1 Hz, 6.4 Hz, 7.2 Hz, 1H), 6.76 (ddd, *J* = 0.8 Hz, 6.4 Hz, 9.2 Hz, 1H), 7.27-7.36 (m, 1H), 7.40-7.58 (m, 5H), 7.80-7.87 (m, 3H), 7.93-7.99 (m, 2H), 8.21 (dt, *J* = 1 Hz, 7.2 Hz, 1H)

^{13}C NMR (50 MHz, $CDCl_3$): δ 113.35, 119.13, 119.83, 121.76, 126.61, 126.85, 127.68, 128.35, 128.78, 128.89, 129.06, 130.06, 131.90, 134.89, 138.06

MS (ESI): m/z 271.33$[M+1]^+$

2-(1-phenylimidazo[1,5-a]pyridin-3-yl)phenol (**3**)

792 mg, yield = 50.7%; solid, m.p.:187°C

^{1}H NMR (200 MHz, $CDCl_3$): δ 5.07 (s, 1H), 6.43 (ddd, *J* = 1.2 Hz, 6.4 Hz, 7.3 Hz, 1H), 6.60 (ddd, *J* = 1 Hz, 6.4 Hz, 9.2 Hz, 1H), 6.77 (ddd, *J* = 1.4 Hz, 7.2 Hz, 7.8 Hz, 1H), 6.96 (ddd, *J* = 0.4 Hz, 1.4 Hz, 8.2 Hz, 1H), 7.03-7.15 (m, 2H), 7.21-7.30 (m, 2H), 7.51 (ddt, *J* = 0.4 Hz, 1.6 Hz, 7.8 Hz, 1H), 7.58-7.68 (m, 3H), 8.22 (dt, *J* = 0.8 Hz, 7.4 Hz, 1H)

^{13}C NMR (50 MHz, $CDCl_3$): δ 113.94, 114.31, 117.94, 119.14, 119.42, 120.65, 122.63, 124.67, 126.81, 127.03, 127.17, 128.94, 129.83, 130.17, 133.65, 135.66, 156.56

HRMS (ESI): m/z calculated for $C_{19}H_{15}N_2O$ $[(M + H^+)]$ 287.1184; found 287.1173.

HRMS (ESI): *m/z* calculated for $C_{19}H_{13}N_2O$ [(M – H] 285.1028 ; found 285.0944.

3-(2-methoxyphenyl)-1-phenylimidazo[1,5-*a*]pyridine (**4**) [17b,c]

810 mg, yield = 61.8%; solid, m.p.:106°C

^{1}H NMR (200 MHz, $CDCl_3$): δ 3.80 (s, 3H), 6.53 (ddd, *J* = 1.2 Hz, 6.4 Hz, 7.2 Hz, 1H), 6.80 (ddd, *J* = 1 Hz, 6.4 Hz, 9.2 Hz, 1H), 7.05 (dd, *J* = 0.8 Hz, 8.4 Hz, 1H), 7.13 (td, *J* = 1 Hz, 7.5 Hz, 1H), 7.24-7.33 (m, 1H), 7.42-7.52 (m, 3H), 7.59 (dt, *J* = 1 Hz, 7.2 Hz, 1H), 7.70 (ddd, *J* = 0.4 Hz, 1.8 Hz, 7.6 Hz, 1H), 7.86 (dt, *J* = 1.2 Hz, 9.4 Hz, 1H), 7.95-8.00 (m, 2H)

^{13}C NMR (50 MHz, $CDCl_3$): δ 55.61, 111.25, 112.15, 118.64, 119.05, 119.67, 121.29, 123.59, 126.35, 126.81, 127.47, 128.70, 130.97, 131.41, 132.88, 135.19, 136.20, 157.47

HRMS (ESI): m/z calculated for $C_{20}H_{17}N_2O$ [(M + H^+)] 301.1341; found 301.1330.

4-(1-phenylimidazo[1,5-a]pyridin-3-yl)benzonitrile (**5**)

1070 mg, yield = 81.6%; m.p.:228°C

^{1}H NMR (200 MHz, $CDCl_3$): δ 6.70 (ddd, *J* = 1.4 Hz, 6.5 Hz, 7.2 Hz, 1H), 6.89 (ddd, *J* = 1 Hz, 6.4 Hz, 9.2 Hz, 1H), 7.29-7.37 (m, 1H), 7.44-7.53 (m, 2H), 7.79 (ddd, *J* = 1.4 Hz, 2 Hz, 8 Hz, 2H), 7.86-7.94 (m, 3H), 8.01 (ddd, *J* = 1.4 Hz, 1.9 Hz, 8.1 Hz, 2H), 8.28 (dt, *J* = 1 Hz, 7.2 Hz, 1H)

^{13}C NMR (50 MHz, $CDCl_3$): δ 111.85, 114.65, 118.70, 119.58, 120.85, 121.58, 127.03, 127.25, 128.27, 128.76, 128.96, 132.86,133.23, 134.14, 134.22, 135.77

HRMS (ESI): m/z calculated for $C_{20}H_{14}N_3$ [(M + H^+)] 296.1187; found 296.1177.

N,*N*-dimethyl-4-(1-phenylimidazo[1,5-a]pyridin-3-yl)aniline (**6**) [14b]

758 mg, yield = 55.3%; m.p.:138°C

^{1}H NMR (200 MHz, CD_3OD): δ 3.04 (s, 6H), 6.66 (t, *J* = 6.8 Hz, 1H), 6.83 (d, *J* = 7.8 Hz, 1H), 6.91 (d, *J* = 8.3 Hz, 2H), 7.31 (t, *J* = 7.3 Hz, 1H), 7.46 (t, *J* = 7.3 Hz, 3H), 7.62 (d, J = 8.4 Hz, 2H), 7.81 (d, *J* = 7.6 Hz, 3H), 8.22 (d, *J* = 7.3 Hz, 1H).

^{13}C NMR (50 MHz, CD_3OD): δ 152.61, 140.53, 135.86, 131.98, 130.57, 129.77, 128.31, 127.99, 127.66, 123.23, 121.27, 119.75, 117.89, 114.58, 113.49, 40.49.

MS (ESI): m/z 314.40$[M+1]^+$

3-(1*H*-indol-3-yl)-1-phenylimidazo[1,5-*a*]pyridine (**7**)

341 mg, yield = 25.3%; m.p.:139°C

^{1}H NMR (200 MHz, CD_3OD): δ 4.54 (s, 1H), 6.53 (t, *J* = 6.4 Hz, 1H), 6.67 (t, *J* = 7.4 Hz, 1H), 7.25-7.03 (m, 3H), 7.47-7.35 (m, 3H), 7.59 (d, J = 7.4 Hz, 1H), 7.83 -7.67(m, 4H), 7.98 (d, *J* = 6.8 Hz, 1H).

^{13}C NMR (50 MHz, CD_3OD): δ 137.95, 136.03, 131.83, 129.78, 128.11, 127.87, 127.55, 127.37, 126.63, 126.59, 123.81, 123.53, 121.33, 121.21, 121.00, 119.68, 114.25, 112.99, 105.39.

HRMS (ESI): m/z calculated for $C_{21}H_{16}N_3$ $[(M + H^+)]$ 310.1344; found 310.1332.

N,*N*-diphenyl-4-(1-phenylimidazo[1,5-*a*]pyridin-3-yl)aniline (**8**)

195 mg, yield = 34.8%; m.p.:155°C

^{1}H NMR (200 MHz, $CDCl_3$): δ 6.54-6.62 (m, 1H), 7.79 (broad, 1H), 7.03-7.34 (m, 14H), 7.47 (t, *J* = 7.4 Hz, 2H), 7.70 (d, *J* = 8.6 Hz, 2H), 7.84 (dt, *J* = 1.2 Hz, 9.2 Hz, 1H), 7.95 (d, *J* = 7.4 Hz, 1H), 8.24 (broad, 1H)

^{13}C NMR (50 MHz, $CDCl_3$): δ 119.39, 120.03, 122.08, 122.16, 123.06, 123.19, 123.75, 125.16, 126.92, 127.03, 127.11, 127.22, 127.41, 128.89, 129.45, 129.57, 138.02, 147.37, 148.87

HRMS (ESI): m/z calculated for $C_{31}H_{24}N_3$ [(M + H^+)] 438.1970; found 438.1953.

3-(naphthalen-1-yl)-1-phenylimidazo[1,5-*a*]pyridine (**9**)

1095 mg, yield = 78.2%; m.p.:160°C

^{1}H NMR (200 MHz, $CDCl_3$): δ 6.49 (t, *J* = 6.8 Hz, 1H), 6.83 (dd, *J* = 6.4 Hz, 9.2 Hz, 1H), 7.28-7.66 (m, 7H), 7.73-7.82 (m, 2H), 7.90-8.04 (m, 5H)

^{13}C NMR (50 MHz, $CDCl_3$): δ 112.78, 118.75, 119.86, 122.02, 125.30, 125.45, 126.26, 126.38, 126.60, 126.95, 127.04, 127.11, 128.49, 128.67, 128.71, 129.88, 131.49, 131.78, 133.86, 135.03, 136.68

MS (ESI): m/z 321.13$[M+1]^+$

1-(1-phenylimidazo[1,5-*a*]pyridin-3-yl)naphthalen-2-ol (**10**)

1053 mg, yield = 71.6%; m.p.:196°C

^{1}H NMR (200 MHz, $CDCl_3$): δ 6.47 (d, *J* = 6.7 Hz, 1H), 6.75(t, *J* = 6.8 Hz, 1H), 7.05 (d, *J* = 8.8 Hz, 1H), 7.24-7.47 (m, 6H), 7.68 (d, J = 8.4 Hz, 1H), 7.74-7.80 (m, 4H), 8.0 (d, *J* = 8.0 Hz, 1H).

^{13}C NMR (50 MHz, $CDCl_3$): δ 155.14, 148.69, 137.21, 134.20, 133.08, 131.73, 131.51, 131.11, 130.81, 128.72, 128.31, 127.12, 126.80, 126.51, 126.31, 124.78, 124.53, 123.57, 120.59, 113.20, 108.17.

HRMS (ESI): m/z calculated for $C_{23}H_{17}N_2O$ [(M + H^+)] 337.1341; found 337.1328.

3-(anthracen-9-yl)-1-phenylimidazo[1,5-*a*]pyridine (**11**)

456 mg, yield= 28.2%; m.p.:202°C

^{1}H NMR (200 MHz, $CDCl_3$): δ 6.41 (t, *J* = 6.8 Hz, 1H), 6.86 (dd, *J* = 6.4 Hz, 9.2 Hz, 1H), 7.17 (d, *J* = 7 Hz, 1H), 7.30-7.56 (m, 9H), 8.03 (d, *J* = 9.4 Hz, 1H), 8.12 (d, *J* = 7.8 Hz, 4H), 8.67 (s, 1H)

^{13}C NMR (50 MHz, $CDCl_3$): δ 113.04, 118.99, 120.09, 122.20, 122.95, 125.57, 125.64, 126.54, 126.75, 127.04, 127.10, 128.84, 129.61, 129.65, 131.51, 131.71, 131.91, 135.14, 135.17

HRMS (ESI): m/z calculated for $C_{27}H_{19}N_2$ [(M + H^+)] 371.1548; found 371.1536.

2.3 **Spectroscopic characterization of the 1-phenylimidazo[1,5-*a*]pyridines**

UV-Vis spectra were recorded on a Shimadzu UV-1700 spectrophotometer using different solvents in order to investigate the solvatochromic behavior of **1-11**: a stock solution ($3.5 \cdot 10^{-3}$ M) in acetonitrile was prepared and diluted solutions ($3.5 \cdot 10^{-5}$ M) in cyclohexane, dichloromethane, acetonitrile, methanol and aqueous solution of HCl 1 M were analyzed.

Fluorescence measurements were recorded using a HORIBA Jobin Yvon Fluorolog 2 (for the excitation wavelengths see Table 3). The wavelength range used for fluorescence emission measurements was between 360 nm and 750 nm. Fluorescence quantum yields were determined using the same instrument with a comparative method [30], using Rhodamine 6G (Φ = 0.94) and Rhodamine 101 (Φ = 0.96) as standards [31-32].

2.4 **Crystal Structure.**

Single crystal data of compounds **2**, **7** and **11** have been collected on a Gemini R Ultra diffractometer and on a X-Calibur Sapphire3 diffractometer [33]. All data were collected using graphite-monochromated Mo Kα radiation (λ = 0.71073). Cell parameters were retrieved using CrysAlisPro [34] software, and the same software was used to perform data reduction with

correction for Lorenz and polarizing effects. Scaling and absorption corrections were applied by CrysAlisPro multi-scan technique. All structures were solved by direct methods using SHELXS-97 [35] and SIR2014 [36] and refined with full-matrix least-squares on F^2 using SHELXL-97 [35]. All non-hydrogen atoms, except disordered moieties in compound **11**, have been refined anisotropically. Hydrogen atoms have been located in the final Fourier-difference maps and refined as riding atoms. Structural pictures have been drawn using CCDC Mercury [37]. Crystal data and structure refinements can be found in Table 2. All the refinement data, the atomic parameters and the tables with angles and distances can be found in SI document. CIF files of the structures have been deposited on the CCDC database with codes 1447690, 1447691 and 1447959.

Table 2.

2.5 **Preparation of polyurethane films with compound 4**

An amount of compound **4** necessary to reach a final concentration of 0.1% w/w in the resin was dissolved in a minimum volume of dichloromethane. To this solution, the two precursors of the polyurethane resin (the polyol, LCR 540RT-DH and the isocyanate, DK 100LV) were added in a 1:1 ratio and mechanically stirred. The mixture was placed in a vacuum bell to evaporate the dichloromethane – leaving compound **4** dissolved in the resin – and to degas the liquid to avoid air bubbles in the final film. To produce the film, a mold was fabricated by Scotch-taping two aluminum bars (to facilitate the film removal) and then placing a spacer of a defined thickness on the long sides of one of the bars to control the film thickness. Once the liquid resin was deposited on the substrate, the substrate was placed again in the vacuum bell for a final outgassing step and

then covered with the second aluminum bar. The mold was finally placed in an oven at 80°C for 30 min to speed up the resin polymerization.

3. Results and Discussion

3.1 **Synthesis**

A one-pot direct cyclization of phenyl(pyridin-2-yl)methanone with eleven different aldehydes in the presence of ammonium acetate in boiling acetic acid was used to obtain compounds **1-11** (Scheme 1). Electron withdrawing and electron donating substituents on the aldehyde were very well tolerated in this reaction. The optimal condition was established to have a 1.0 : 1.5 : 5 molar ratio of ketone/aldehyde/ammonium acetate.

Scheme 1.

The isolated yields vary from moderate (28.2% for **11)** to excellent (81.6% for **5**).

3.2 **Optical characteristics of the compounds**

Good absorption properties in a selected spectral region and efficient emission properties with large Stokes' shifts are fundamental requirements for any organic emitter, designed to be used in luminescent down-shifting (LDS) layers [4]. Our substituted 1-phenylimidazo[1,5-*a*]pyridines show absorption maxima below 400 nm, with a good transparency in the visible range, and a wide variety of fluorescent emissions at wavelengths in the range of 467-562 nm, thus resulting

in a large Stokes' shift, as can be seen in Table 3, where the main optical parameters for all molecules in CH_2Cl_2 are reported.

Table 3.

3.2.1 Absorption properties

The main absorption peaks were observed in the wavelength range between 300 nm and 382 nm, with almost no absorption beyond 450 nm. Usually, the compounds presented two main bands, one in the 300-320 nm range (except compounds **3** and **5**) and a second one centered at 360-380 nm. The intensity of the absorption significantly increased going from compound **1** (methyl substituent in position 3) to **2-11**, as a clear consequence of the hyperchromic effect induced by the extension of the conjugation due to the aromatic substituent in position 3.

The various substituents had a definite effect on the absorption bands. It was evident that both electron-donating (i.e. $N(CH_3)_2$ group, compound **6**) and electron-withdrawing groups (i.e. CN group, compound **5**) on a phenyl substituent in position 3 had a strong and opposite effect on the absorption behavior in the 360-380 nm range, compared to the parent phenyl group (Figure 2, Top-Left). Compound **4**, having a donor methoxy group instead of a hydroxyl group, showed a different behavior in respect to compound **3**.

Figure 2.

In Figure 2 (Top-Right) the absorption spectra of 3-substituted 1-phenylimidazo[1,5-*a*]pyridines with methyl (compound **1**), phenyl (compound **2**), naphthalene (compound **9**) and anthracene

(compound **11**) groups were compared. The extension of the conjugation system was evident in the evolution of the ratio between the intensity of the peak at high energy (308 nm), and the second band at 360-390 nm.

Figure 2 (Bottom-Left) shows the absorption spectra of compounds **1**, **2**, **7**, **8** to compare the effect of different substituents in position 3. In comparison to reference dyes (**1** and **2**), an evident hyperchromic effect was shown for compound **8** at low energy, while the indole group induced a hypochromic effect over 350 nm.

The presence of the hydroxyl group in compounds **3** and **10** increased the intensity of the absorption in respect to the analogous dyes **2** and **9** without hydroxyl group (Figure 2, Bottom-right).

The light harvesting properties of these compounds were also studied in a series of solvents with different polarity, to assess the effect of the chemical environment. The resulted spectra showed very little changes with increasing solvent polarity in non protic systems, indicating that there is practically no charge transfer effect even in the presence of a strong electron donor (i.e. OCH_3, compound **4**) or of a strong electron acceptor (CN, compound **5**), as stated in Table 3. In Figure 3, spectra of compound **3** in different solvents are reported as an example. This behavior is of particular interest because it demonstrates the possibility to host this class of molecules in several polymers without an appreciable change in their photophysical response.

Conversely, in the case of protic solvents and aqueous solutions at different pH, the absorption profile was significantly different. This behavior was common to all studied compounds, which lead to the conclusion that the common moiety imidazo[1,5-*a*]pyridine was most likely responsible for this difference [38]. Insertion of the molecules in polar matrixes might thus result in varied photophysical properties.

Figure 3.

3.2.2 Emission properties

The emission spectra of compounds **1-11** in dichloromethane solution are showed in Figures 4-6 and their emission wavelengths are reported in Table 3. Most of the products showed an emission band centered between 470 nm and 500 nm. The emission of compound **11** bearing an anthracene moiety, which occurred 80 nm bathocromically shifted (Figure 4a), respect to the other compounds, resulted particularly interesting. In the case of a substitution with an indole (compound **7**) or a triphenylamine (compound **8**), emission data showed moderate bathochromic shifts (15-20 nm) compared to the reference dyes **1** and **2** (Figure 4b).

Figure 4.

The presence of a substituent on the phenyl moiety (compounds **2**-**6**) had little influence on the emission spectra. These results showed that electron-donating group strength and position did not modify the emission maximum, while a small bathochromic shift was observed in compound **6**, bearing and electron donor group (Figure 5).

Figure 5.

Stokes' shifts of compounds **1-11** were strongly influenced by the group bonded to the imidazo[1,5-*a*]pyridine ring. The extension of the conjugation system in the side group increased the Stokes' shift from 99 nm for the phenyl in compound **2**, to 129 nm for the naphthalene in compound **9** and to 166 nm for the anthracene in compound **11**. There was also a clear effect of the substituent on the phenyl ring. Compound **5**, bearing a CN group, showed the smallest Stokes' shift, while compound **6**, bearing a dimethylamino group in the same position, showed a Stokes' shift up to 123 nm. The substituent influenced the fluorescence intensities. The 2-methoxyphenyl group (compound **4**) showed the maximum quantum yield ($\Phi = 0.385$), which, to our knowledge, is also the highest reported in literature among the imidazo[1,5-*a*]pyridines. With the exception of the methoxy group of compound **4**, all other substituent groups in position 3 on the phenylimidazo[1,5-*a*]pyridine skeleton decreased the quantum yield compared to the methyl group of compound **1** ($\Phi = 0.263$) with the lowest yield observed in presence of the anthracene mojety ($\Phi = 0.064$).

As already discussed in the introduction section, compounds **3** and **10**, bearing a hydroxyl group in the ortho position of the 3-phenyl substituent, were intentionally synthesized in order to verify a possible ESIPT effect on the emission properties. However, the comparison among the quantum yields and emission spectra of compounds **2, 3** and **9, 10** highlighted the absence of interactions between the hydroxyl group in the o-cresol and the naphthalen-2-ol substituents and the 2-nitrogen of the imidazo[1,5-*a*]pyridine. The emission spectrum of the 2-naphthol group (compound **10**) was shifted of about 20 nm compared to the naphthalene substituent (compound **9**), while the comparison between the phenyl (compound **2**) and the phenol (compound **3**) group indicated no difference (Fig. 6).

Figure 6.

The solvent effect on the fluorescence behavior of all compounds was studied. Spectra of compound **3** are reported as an example (Figure 7). Regarding the emission spectra, all compounds showed a structured emission in cyclohexane solution around 450 nm with its vibronic bands at about 480 nm and 510 nm. No significant differences were observed in the emission peak maxima in both protic and aprotic solvents, while the acid aqueous solution showed a significantly different profile. This interesting behavior is promising for a possible use of this class of molecules as pH sensors [38].

Figure 7.

Table 4.

Table 5.

3.4 **Crystal Structure Analysis**

Compound **2** crystallized after slow evaporation of acetone in the orthorhombic non-centrosymmetric space group $Cmc2_1$ (see Fig. 8). This non-centrosymmetric space group was rather unexpected, since compound **2** does not have any chiral center. It is worth pointing out that, we attempted the solution of the structure both in symmetries lower than orthorhombic and

in the centrosymmetric orthorhombic Cmcm but no solution was found. The R value was rather good in $Pn2_1a$, similarly to $Cmc2_1$and the correlation coefficients and thermal factor showed no anomalies, typically observed in the case of a wrong space group. The higher symmetry non-centrosymmetric space group (i.e. $Cmc2_1$) with good agreement values was finally chosen. It must be noticed that a non-centrosymmetric group is sometimes observed in non-chiral molecules due to the crystal packing, as already observed for this class of compounds [21e]. The asymmetric unit contains only half molecule; the entire molecule is generated by a symmetry plane passing through the N2 atom and the N1-C3 bond. This symmetry implies an overall positional disorder in the molecule, with two different positions for the N1/C3 atoms, constrained to the same probability and both labelled in the same position in Figure 11a. The overall crystal packing is substantially driven by Van der Waals interactions, since steric hindrance of the phenyl moieties does not permit the π-π stacking of the aromatic systems. Compound **4**, used for dispersion in the polymeric resin, is very similar (only a methoxy group is added) to compound **2**, and it can be inferred that similar weak interactions characterize its packing and clustering behavior. The presence of weak and non-polar interactions explains its easy dispersion into the polyurethane resin, to produce a photoactive polymer. The main molecule-polymer interactions should consist of the same weak contacts involving the aromatic rings. However, looking at the molecular structure of **2** (Figure 8a), the nitrogen atom should be accessible enough to accept weak CH•••N bonds when **4** is dispersed into polyurethane resin.

Figure 8.

Figure 9.

Figure 10.

Compound **7** crystallized from dichloromethane in yellow crystals in the monoclinic space group $P2_1/c$. Two different non-equivalent molecules of the product and two disordered molecules of the solvent co-crystallized during the crystal growth, as can be seen in the asymmetric unit (Figure 9a). This disorder might explain the weak diffracting nature of this crystal. The overall structure is built up by chains based on hydrogen bonds through the *N*-indolic hydrogen and the imidazolic nitrogen of the imidazopyridine central backbone of the vicinal molecules (Figure 9b). These chains are isolated by the presence of the solvent molecules that seem not involved in weak NH•••Cl hydrogen bonds. The presence of the phenyl group generates a separation of the chains in layers bonded by dispersion forces only, without the presence of π-π stacking due to the relevant steric hindrance. These relatively strong H-bonds are not perturbed by dichloromethane and presumably also by other polar solvents. It might be inferred that the NH•••Cl interaction is maintained also in solution of different polarity, thus explaining the similar position of emission maxima in polar solvents (see Table 5) for compound **7**.

Crystals of compound **11** were grown by slow evaporation of a dimethyl ether solution. All tested crystals resulted twinned. In the best dataset, the presence of three individuals was recognized (Table 2S) and twinning was treated by CrysAlisPro. In the measured sample one individual was largely predominant and the simultaneous refinement of the four individuals with the HKLF 5 option resulted unstable, so this method was discarded. The refinement was thus completed on the extracted HKLF4.hkl file of the predominant individual. The structure was initially solved in Pn, then an additional 2-fold screw axis was found by PLATON [39] and the

space group changed in the more common centrosymmetric P21/n. The phenyl ring is free to oscillate, as indicated by the presence of disorder that was treated using the PART command.

Compound **11** crystallized in a cell with two angles of 90° and the β angle close to 90° (Fig.10). The crystal system is thus monoclinic but almost orthorhombic, with a lattice parameter a≈1/2b≈1/2c. The individuals grew by exchanging "b" and "c", which were similar, and occasionally doubling the packing along "a", as can be inferred from the orientation matrices reported in table 2S in the SI file. The twinning, occurring through the above mentioned axes exchange, was thus favored by the absence of directional interactions in the packing, held only by weak interactions such as T-shape CH-π contacts. These contacts should also be favored in polar solvent, inducing a molecular clustering, while in apolar solvents they should be overwhelmed by solute-solvent interaction, with a more efficient dispersion. Such different dispersion efficiency might contribute to the explanation of the different spectroscopic behavior in different solvents. In fact, as can be seen in Table 4 and 5, the different solvents induce different positions of the emission maximum.

3.5 **Optical properties in a polymer host**

Based on the data in Table 3, compound **4** was selected as a possible candidate for down-shifting applications, due to the much higher quantum yield compared to the other molecules of the series. This approach has also been recently proposed on another class of low cost fluorophores [40].

To assess the photophysical properties of compound **4** for down-shifting applications, films with the compound uniformly dissolved inside a polymeric medium were produced, in order to evaluate its properties in the solid state. A commercial polyurethane resin already used for

photovoltaic and lighting devices was used to produce a luminescent polymer (see Fig.12). Spectra of such films are reported in Figure 11 and show that the absorption in the solid state did not change compared to the dichloromethane solution, while the emission was blue-shifted of about 15 nm when compared to the solution. Despite this blue shift, the overlap between the absorption and emission peaks in the solid state resulted still negligible, which means that there will be very little re-absorption of the emitted light from the compound itself.

Figure 11.

Figure 12.

4. Conclusions

Eleven 1,3-diarylated imidazo[1,5-*a*]pyridine derivatives were synthesized by means of the easy to scale up one-pot condensation of phenyl(pyridin-2-yl)methanone with several aldehydes and ammonium acetate. Reaction yields were moderate to excellent (from 28.2% for **11** to 81.6% for **5**). All the phenylimidazo[1,5-*a*]pyridines obtained exhibited interesting optical properties in solution, with a wide variety of fluorescent emissions (467-548 nm). These compounds showed large Stokes' shifts and, depending on the chemical structure of the substituent in position 3, fluorescence quantum yields (Φ) in solution were easily tuned from 6.4% (compound **11**) to 38.5% (compound **4**). From the results of the optical studies we excluded the ESIPT fluorescence mechanism in all the products. The crystal structures of **2**, **7** and **11** were also solved, in order to

gain insights about the intermolecular interactions, and their effect on the optical properties in solution and when dispersed into a polymeric resin.

Finally, compound **4**, showing the best compromise between stoke shift and high Φ, was dissolved in a polyurethane resin to investigate its properties in the solid state. Despite a blue shift of 15 nm when compared to a dichloromethane solution, the overlap between the absorption and emission spectra was negligible, proving that it is an interesting low cost candidate for down-shifting applications, also thanks to its large solubility and homogeneous dispersion in the polymer.

On the basis of these promising emission properties, further studies are in progress to test these phenylimidazo[1,5-*a*]pyridines derivatives as tunable low-cost fluorescent materials.

Acknowledgements

This work was supported by Piedmont Region FINPIEMONTE POR-FESR 2007/2013 project "Dye Hard". Dott. A. Menozzi and S.E. are acknowledged for the collaboration, fruitful discussion and providing of polyurethane resin.

References

[1] Niklaus L, Dakhil H, Kostrzewa M, Coto PB, Sonnewald U, Wierschem A, Costa RD. Easy and versatile coating approach for long-living white hybrid light-emitting diodes. Mater Horiz, 2016: DOI: 10.1039/C6MH00038J.

[2] (a) Klampaftis E, Ross D, McIntosh KR, Richards BS. Enhancing the performance of solar cells via luminescent down-shifting of incident spectrum: A review. Sol Energy Mater Sol Cells, 2009;93:1182–1194.

(b) Griffini G, Bella F, Nisic F, Dragonetti C, Roberto D, Levi M, Bongiovanni R, Turri S. Multifunctional Luminescent Down-Shifting Fluoropolymer Coatings: A Straightforward Strategy to Improve the UV-Light Harvesting Ability and Long-Term Outdoor Stability of Organic Dye-Sensitized Solar Cells. Advanced Energy Materials, 2015;5:1401312-9.

(c) Bella F, Griffini G, Gerosa M, Turri S, Bongiovanni R. Performance and stability improvements for dye-sensitized solar cells in the presence of luminescent coatings. Journal of Power Sources, 2015;283:195-203.

[3] Currie MJ, Mapel JK, Heidel TD, Goffri S, Baldo MA. High-efficiency organic solar concentrators for photovoltaics. Science, 2008;321:226-228.

[4] Alonso-Álvarez D, Ross D, Klampaftis E, McIntosh KR, Jia S, Storiz P, Stolz T, Richards BS. Prog Photovoltaics, 2015;23:479-497.

[5] (a) McIntosh KR, Lau G, Cotsell JN, Hanton K, Batzner DL, Bettiol F, et al. Increase in External Quantum Efficiency of Encapsulated Silicon Solar Cells from a Luminescent Down-Shifting layer. Progress in Photovoltaics: Research and Applications, 2009;17:191-7. (b) Klampaftis E, Congiu M, Robertson N, Richards BS. Luminescent Ethylene Vinyl Acetate

Encapsulation Layers for Enhancing the Short Wavelength Spectral Response and Efficiency of Silicon Photovoltaic Modules. IEEE J of Photovoltaics, 2011; 1:29-36.

[6] (a) Joule JM, Mills K. XXX. In: Editors. Heterocyclic Chemistry, Oxford: Black Science; 2000, p. 2xx-3yy.

(b) Knueppel D, Martin SF. Total Synthesis of Cribrostatin 6. Angew Chem Int Ed 2009;48:2569-71.

(c) Kundu N, Maity M, Chetterjee PB. Reporting a Unique Example of Electronic Bistability Observed in the Form of Valence Tautomerism with a Copper(II) Helicate of a Redox-Active Nitrogenous Heterocyclic Ligand. J Am Chem Soc 2011;133:20104-7.

[7] (a) El Khadem HS, Kawai J, Swartz DL. El Khadem HS, Kawai J, Swartz DL. Synthesis of nitrogen-bridged purine-like C-nucleosides from ethyl 2,5-anhydro-6-O-benzoyl-d-allonodithioate. Carbohydr Res 1989; 189:149-60.Carbohydr Res 1989;189:149-60.

(b) Montgomery JA. Secrist III, In: A. R. Katritzky and C. W. Rees, Eds., Comprehensive Heterocyclic Chemistry, Pergamon Press, Oxford, 1984.

c) Degoey DA, Flentge CA, Flosi WJ, Grampovnik DJ, Kempf DJ, Klein LL, Yeung MC, Randolph JT, Wang XC, Yu SUS. Pat Appl Publ U.S. 2005148623; Chem Abstr 2005; 143:133693.

[8] (a) Kim D, Wang L, Hale JJ, Lynch CL, Budhu RJ, MacCoss M,ET AL. Bioorg Med Chem Lett 2005; 15:2129.

(b) Kimura K, Tsuchiya E, Shibahara F, Murai T. Jpn. Kokai Tokkyo Koho JP2008105963; Chem Abstr 2008; 148:509911.

[9] Davey D, Erhardt PW, Lumma WC, Wiggins J, Sullivan M, Pang D, Cantor E. Novel 8-aryl substituted imidazo[1,2-a]- and -[1,5-*a*]pyridines and imidazo[1,5-*a*]pyridinones as potential positive inotropic agents. J Med Chem 1987; 30:1337-42.

[10] Browne LJ, Gude C, Rodriguez H, Steele RE, Bhatnager A. Fadrozole hydrochloride: a potent, selective, nonsteroidal inhibitor of aromatase for the treatment of estrogen-dependent disease. J Med Chem 1991;34:725-36.

[11] Ford NF, Browne LJ, Campbell T, Gemenden C, Goldstein R, Gude C, Wasley JWF. Imidazo[1,5-*a*]pyridines: a new class of thromboxane A2 synthetase inhibitors. J Med Chem 1985;28:164-70.

[12] (a) Nakamura H, Yamamoto H, PCT Int. Appl. WO 2005043630. Chemical Abstracts 2005, 142, Article ID: 440277.

(b) Horowitz G. Organic field-effect transistors. Adv Mater 1998;10:365-77.

[13] (a) Nakatsuka M, Shimamura T. Jpn. Kokai Tokkyo Koho JP 2001035664. Chem Abstr 2001; 134:170632.

(b) Tominaga G, Kohama R, Takano A. JP 2001006877.

(c) Tominaga G, Kohama R, Takano A. Jpn. Kokai Tokkyo Koho JP 2001006877; Chem Abstr 2001;134:93136.

(d) Salassa L, Garino C, Albertino A, Volpi G, Nervi C, Gobetto R, Hardcastle KI. Computational and Spectroscopic Studies of New Rhenium(I) Complexes Containing Pyridylimidazo[1,5-*a*]pyridine Ligands: Charge Transfer and Dual Emission by Fine-Tuning of Excited States. Organometallics 2008;27:1427–35.

(e) Kitazawa D, Tominaga G, Takano A, Jpn. Kokai Tok-kyo Koho JP 2001057292, Chemical Abstracts 2001, Vol. 134, Article ID: 200276.

(f) Chou PT, Chi Y. Phosphorescent Dyes for Organic Light-Emitting Diodes. Chem Eur J 2007;13:380–95.

(g) Weber M. D, Garino C, Volpi G, Casamassa E, Milanesio M, Barolo C, Costa R. D. Origin of a counterintuitive yellow light-emitting electrochemical cell based on a blue-emitting heteroleptic copper(I) complex. Dalton Trans., 2016;45:8984-899.

[14] (a) Yamaguchi E, Shibahara F, Murai T. 1-Alkynyl- and 1-Alkenyl-3-arylimidazo[1,5-*a*]pyridines: Synthesis, Photophysical Properties, and Observation of a Linear Correlation between the Fluorescent Wavelength and Hammett Substituent Constants. J Org Chem 2011;76:6146-58.

(b) Yamaguchi E, Shibahara F, Murai T. Direct Sequential C3 and C1 Arylation Reaction of Imidazo[1,5-*a*]pyridine Catalyzed by a 1,10-Phenanthroline–Palladium Complex. Chem Lett 2011;40:939-40.

[15] (a) Shibahara F, Yamaguchi E, Kitagawa A, Imai A, Murai T.Synthesis of 1,3-diarylated imidazo[1,5-*a*]pyridines with a combinatorial approach: metal-catalyzed cross-coupling reactions of 1-halo-3-arylimidazo[1,5-*a*]pyridines with arylmetal reagents. Tetrahedron 2009;65:5062-73.

(b) Shibahara F, Sugiura R, Yamaguchi E, Kitagawa A, Murai T. Synthesis of Fluorescent 1,3-Diarylated Imidazo[1,5-*a*]pyridines: Oxidative Condensation−Cyclization of Aryl-2-Pyridylmethylamines and Aldehydes with Elemental Sulfur as an Oxidant. J Org Chem 2009;74:3566-8.

[16] (a) Gobetto R, Caputo G, Garino C, Ghiani S, Nervi C, Salassa L, Rosenberg E, Alexander JB Ross, Viscardi G, Martra G, Miletto I, Milanesio M. Synthesis, Electrochemical and Electrogenerated Chemiluminescence Studies of Ruthenium (II)bis(2,2'-bipyridyl)(2-(4-methylpyridin-2-yl)benzo[d]-X-azole) Complexes. Eur J Inorg Chem, 2006;2839-49.

(b) Albertino A, Garino C, Ghiani S, Gobetto R, Nervi C, Salassa L, Rosenberg E, Viscardi G, Croce G, Milanesio M. Photophysical Properties And Computational Investigations Of Tricarbonylrhenium(I)[2-(4-Methylpyridin-2-Yl)Benzo[D]-Xazole] L And Tricarbonylrhenium(I)[2-(Benzo[D]-X-Azol-2-Yl)-4-Methylquinoline]L Derivatives (X = N-Ch3, O, Or S; L = Cl-, Pyridine). J Organomet Chem, 2007;692:1377-91.

[17] (a) Huiqiao W, Wentao X, Zhiqiang W, Lintao Y, Kun X. Copper-Catalyzed Oxidative Amination of sp3 C–H Bonds under Air: Synthesis of 1,3-Diarylated Imidazo[1,5-*a*]pyridines. J Org Chem 2015;80:2431-5.

(b) Nguyen HTH, Nguyen OTK, Truong T, Phan NTS. Synthesis of imidazo[1,5-a]pyridines via oxidative amination of the C(sp3)–H bond under air using metal–organic framework Cu-MOF-74 as an efficient heterogeneous catalyst. RSC Adv. 2016; 6: 36039-49.

(c) Joshi A, Mohan DC, Adimurthy S. Copper-Catalyzed Denitrogenative Transannulation Reaction of Pyridotriazoles: Synthesis of Imidazo[1,5-a]pyridines with Amines and Amino Acids Org. Lett. 2016; 18 (3): 464-7.

[18] (a) Krapcho AP, Powell JR. Syntheses of 1,3-disubstituted imidazo[l,5-a]pyridines. Tetrahedron Lett 1986;27:3713-4.

(b) Hlasta D. Regiospecific Acylation Reactions of Imi-dazo[1,5-*a*]pyridine. Tetrahedron Letters 1990;31:5833-4.

[19] Grigg R, Kennewell P, Savic V, Sridharan V. X=Y-ZH Systems as potential 1,3-dipoles. Part 38. 1,5-Electrocyclisation of vinyl-and iminyl-azomethine ylides. 2-Azaindolizines and pyrrolo-dihydro-isoquinolines. Tetrahedron 1992;48:10423-30.

[20] (a) Bluhm ME, Ciesielski M, Görls H, Döring M. Copper-Catalyzed Oxidative Heterocyclization by Atmospheric Oxygen. Angew Chem Int Ed 2002;41:2962-5.

(b)Yan Qing Ge, Ben Qian Hao, Gui Yun Duan, Jian Wu Wang. The synthesis, characterization and optical properties of novel 1,3,4-oxadiazole-containing imidazo[1,5-*a*]pyridine derivatives. Journal of Luminescence 2011;131:1070-6.

[21] (a) Wang J, Dyers L, Mason R, Amoyaw P, Bu XR. Highly Efficient and Direct Heterocyclization of Dipyridyl Ketone to N,N-Bidentate Ligands. J Org Chem 2005;70:2353-6.

(b)Wang J, Mason R, van Derveer D, Feng K, Bu XR. Convenient Preparation of a Novel Class of Imidazo[1,5-*a*]pyridines: Decisive Role by Ammonium Acetate in Chemoselectivity. J Org Chem 2003; 68:5415-81.

(c)Siddiqui SA, Potewar TM, Lahoti RJ, Srinivasan KV. From the Methods in Organic Synthesis Da-tabase, Synthesis, Vol. 127, 2006,2849-54.

(d)Rahmati A, Khalesi Z. One-Pot Three-Component Synthesis of Imidazo[1,5-*a*]pyridines. Int J Org Chem 2011;1:15-9.

(e) Volpi G, Garino C, Conterosito E, Barolo C, Gobetto R, Viscardi G. Facile synthesis of novel blue light and large Stoke shift emitting tetradentate polyazines based on imidazo[1,5-*a*]pyridine. Dyes and Pigments, 2016;128:96-100.

[22] (a) Demchenko AP, Tang KC, Chou PT. Excited-state proton coupled charge transfer modulated by molecular structure and media polarization. Chem Soc Rev 2013;42:1379-08.

(b) Zhao J, Ji S, Chen Y, Guo H, Yang P. Excited state intramolecular proton transfer (ESIPT): from principal photophysics to the development of new chromophores and applications in fluorescent molecular probes and luminescent materials, Phys Chem Chem Phys 2012; 14:8803–17.

[23] Tanaka H, Tokito S, Taga Y, Okada A. Novel hole-transporting materials based on triphenylamine for organic electroluminescent devices. Chem Commun 1996;18:2175-6.

[24] Moylan CR, Twieg RJ, Lee VY, Swanson SA, Betterton KM, Miller RD. Nonlinear optical chromophores with large hyperpolarizabilities and enhanced thermal stabilities. J Am Chem Soc 1993;115:12599-600.

[25] Rumi M, Ehrlich JE, Heikal AA, Perry JW, Barlow S, Hu Z., et al. Structure−Property Relationships for Two-Photon Absorbing Chromophores: Bis-Donor Diphenyl Polyenes and Bis(styryl)benzene Derivatives. J Am Chem Soc 2000;122:9500-10.

[26] Bellmann E, Shaheen SE, Grubbs RH, Marder SR, Kippelen B, Peyghambarian N. Organic Two-Layer Light-Emitting Diodes Based on High-Tg Hole-Transporting Polymers with Different Redox Potentials. Chem Mater 1999;11:399-407.

[27] Crawforth JM, Paoletti M. A one-pot synthesis of imidazo[1,5-*a*]pyridines. Tetrahedron Letters 2009;50:4916-8.

[28] Chiassai L, Adam R, Drechslerovà M, Ballesteros R, Abarca B. Approaches for the introduction of fluorinated substituents into [1,2,3]Triazolo[1,5-*a*]pyridines. J Fluorine Chem 2014;164:44-50.

[29] Li M, Xie Y, Ye Y, Zou Y, Jiang H, Zeng W. Cu(I)-Catalyzed Transannulation of N-Heteroaryl Aldehydes or Ketones with Alkylamines via C(sp3)–H Amination. Org Lett 2014;16:6232-3.

[30] Williams ATR, Winfield SA, Miller JN. Relative fluorescence quantum yields using a computer-controlled luminescence spectrometer. Analyst 1983;108:1067–71.

[31] Brouwer AM. Standards for photoluminescence quantum yield measurements in solution (IUPAC Technical Report). Pure Appl Chem 2011;83:2213-28.

[32] Jobin Yvon Ltd., A Guide to Recording Fluorescence Quantum Yields-Application Note, 1996,

www.horiba.com/fileadmin/uploads/Scientific/Documents/Fluorescence/quantumyieldstrad.pdf.

[33] Agilent Technologies UK Ltd., Oxford, U.K.

[34] Agilent Technologies 20129. CrysAlisProSoftare system, version 1.171.35.11, Agilent Technologies U K Ltd., Oxford, U.K.

[35] Sheldrick, G.M., SHELX97: Program for Crystal Structure Solution and Refinement; University of Göttingen: Göttingen, Germany, 2004.

[36] Burla MC, Caliandro R, Carrozzini B, Cascarano GL, Cuocci C, Giacovazzo C, et al. Crystal structure determination and refinement via SIR2014. J Appl Cryst 2015;48:306–9.

[37] Macrae CF, Edgington PR, McCabe P, Pidcock, E, Shields GP, Taylor R, et al. Mercury: visualization and analysis of crystal structures. J Appl Crystallogr 2006;39:453–7.

[38] Hutt JT, Jo J, Olasz A, Chen C-H, Lee D, Aron ZD. Fluorescence Switching of Imidazo[1,5-*a*]pyridinium Ions: pH-Sensors with Dual Emission Pathways. Org Lett, 2012;14:3162–3165.

[39] Spek AL, PLATON A Multipurpose Crystallographic Tool, Utrecht University, Utrecht, Holland, 2008.

[40] Conterosito E, Benesperi I, Toson V, Saccone D, Barbero N, Palin L, Barolo C, Gianotti V, Milanesio M. High-Throughput Preparation of new Photoactive nanocomposites. ChemSusChem, 2016, 9 (11): 1279-89.

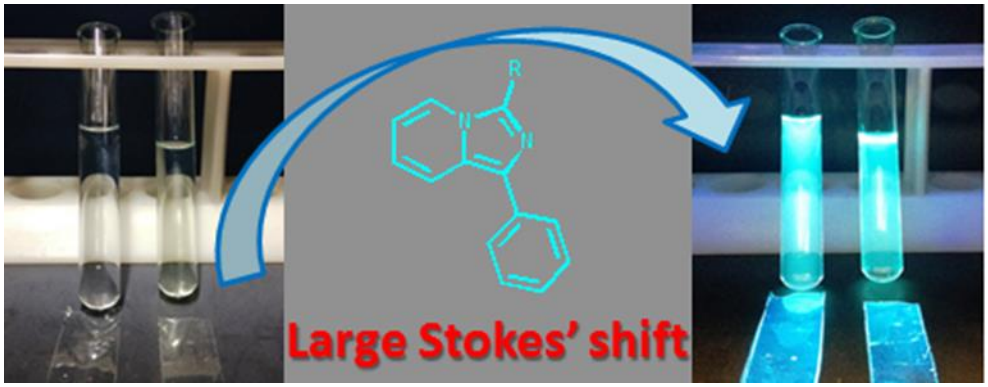
R
N
Large Stokes' shift

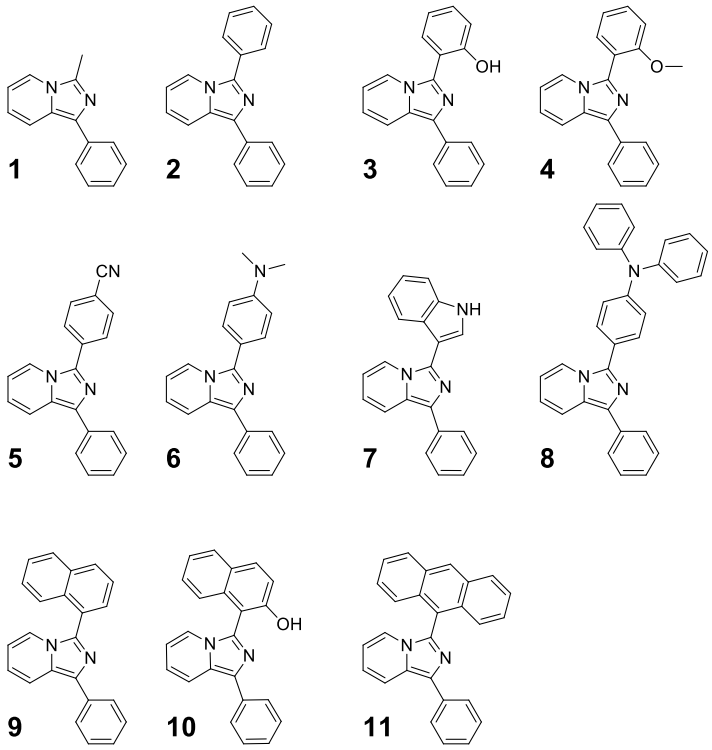

Fig. 1. 3-substituted-1-phenylimidazo[1,5-*a*]pyridines.

Table 1. Comparison of different synthetic approaches for compounds **1**, **2**, **4**, **6** and **9** previously reported.

COMPOUNDS	CATALYST	LITERATURE YIELD %	OXIDANT Or DEYHDRATING	REFERENCES
1	NO	82	YES (T3P)	[27]
	NO	6	NO	[28]
	NO	78	NO	This work
2	YES (Ni)	99	NO	[15b]
	NO	74	Yes (S_8)	[15b]
	YES (Cs/Pd)	74	NO	[14b]
	Yes (Cu)	42	NO	[29]
	YES (Cu)	93	NO	[17]
	NO	81	NO	This work
4	YES (Cu MOF74)	61	NO	[17b]
	YES (Cu)	65	NO	[17c]
	NO	62	NO	This work
6	YES (Cs/Pd)	71	NO	[14b]
	NO	55	NO	This work
9	YES (Cu)	90	NO	[17]
	NO	78	NO	This work

Table 2. Crystal data and structure refinement for compounds **2**, **7** and **11**.

Compound	**2**	**7**	**11**
Crystal system, space group	Orthorhombic, Cmc2(1)	Monoclinic, P2(1)/c	Monoclinic P2(1)/n
Unit cell dimensions (Å and °)	a = 23.840(1) b = 7.4163(3) c = 7.8802(3)	a = 19.230(1) b = 9.5164(5) c = 22.460(1) β = 107.03(1)	a = 8.062(2) b = 16.292(8) c = 14.341(3) β = 90.37(2)°
Volume ($Å^3$)	1393.29(9)	3929.9(4)	1883.6(12)
Reflections collected / unique	10783 / 1463 [R(int) = 0.0309]	30388 / 5635 [R(int) = 0.0695]	32724 / 3187 [R(int) = 0.0517]
Final R indices [I>2sigma(I)]	R1 = 0.0318 wR2 = 0.0773	R1 = 0.0591 wR2 = 0.1399	R1 = 0.0467 wR2 = 0.1295
Largest diff. peak and hole (e $Å^{-3}$)	0.130 and -0.229	0.348 and -0.247	0.182 and -0.172

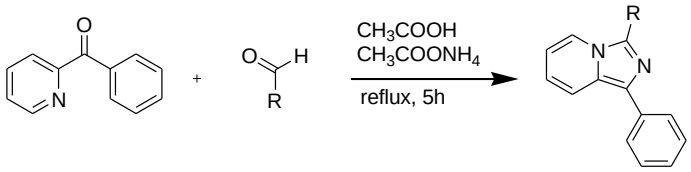

Scheme 1. One-pot synthesis of substituted 1-phenylimidazo[1,5-*a*]pyridines

Table 3. Selected photophysical properties of the obtained 1-phenylimidazo[1,5-*a*]pyridines in dichloromethane solution.

	Absorption		**Emission**			
Compound	**λ_{abs} (nm)**	**ε (M^{-1} cm^{-1})**	**λ_{ex} (nm)**	**λ_{em} (nm)**	**Φ_F (%)**	**Stokes' shift (nm)**
1	306 367	7525 3113	367	485	26.3	118
2	306 342sh 385sh	19958 12215 5215	385	484	21.7	178
3	316 345	16587 17990	345	484	14.4	139
4	305 374sh	23664 7953	374	479	38.5	174
5	301 380	17169 22208	380	477	21.0	97
6	316 372	19846 3290	372	495	12.0	123
7	309 380	13639 3161	380	506	16.2	126
8	305 353	31688 30783	353	491	12.7	138

9	305 357	17507 10842	357	486	12.5	129
10	306 314sh 362	11578 10495 10634	362	467	13.6	105
11	304 366 382	17090 14213 14255	366	548	6.4	166

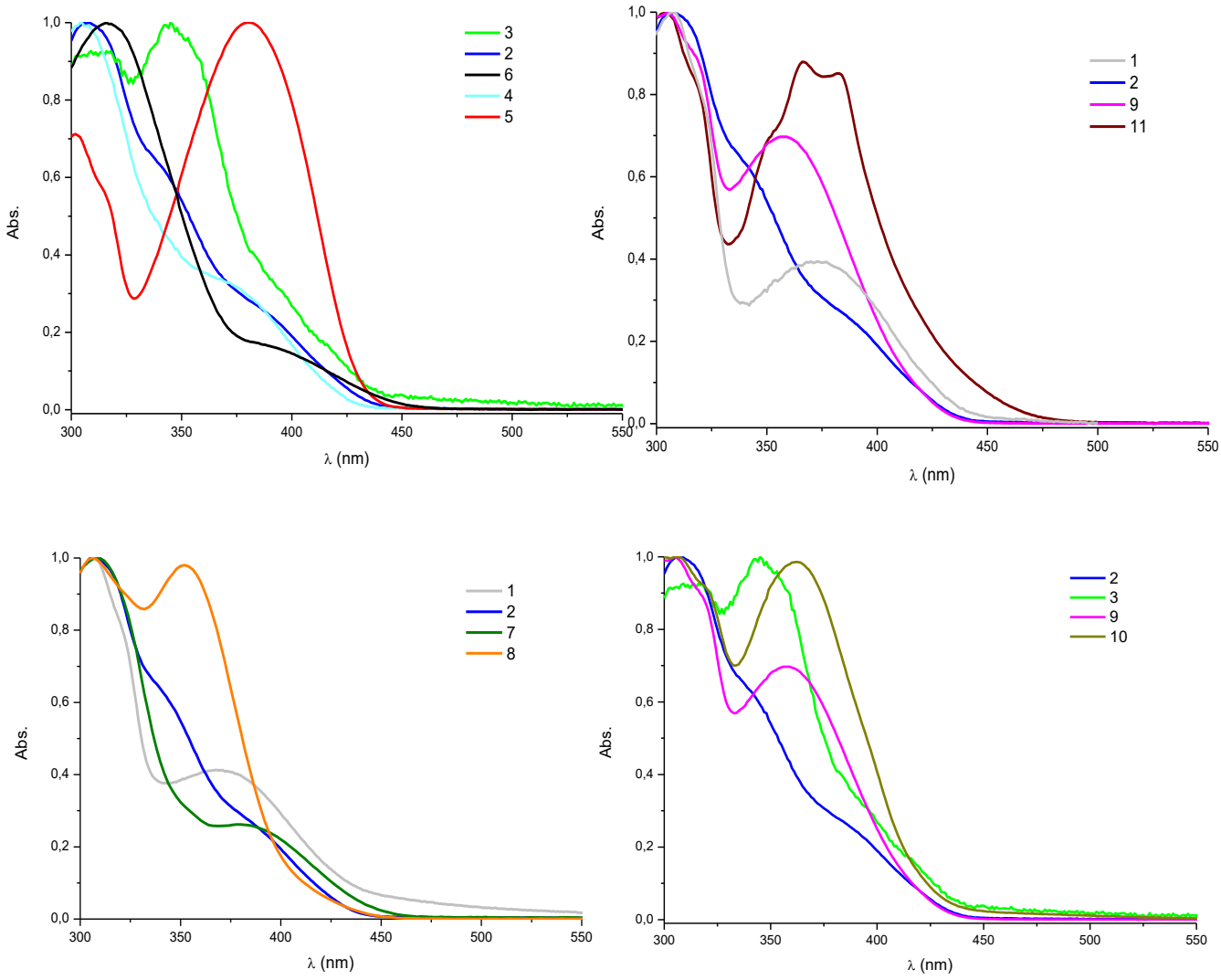

Fig. 2. Comparison between UV-Visible spectra of compounds **1-11** in dichloromethane. Top-Left: Compounds 2-6 Top-Right: Compounds 1, 2, 9, 11 Bottom-Left: Compounds 1, 2, 7, 8. Bottom-Right: Compounds 2, 3, 9 and 10.

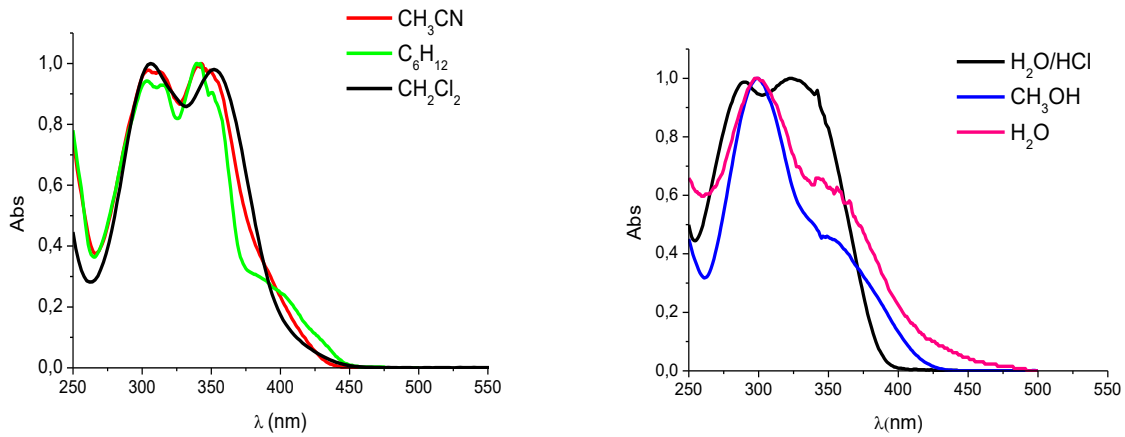

Fig. 3. Absorption spectra of **3** in different solvents.

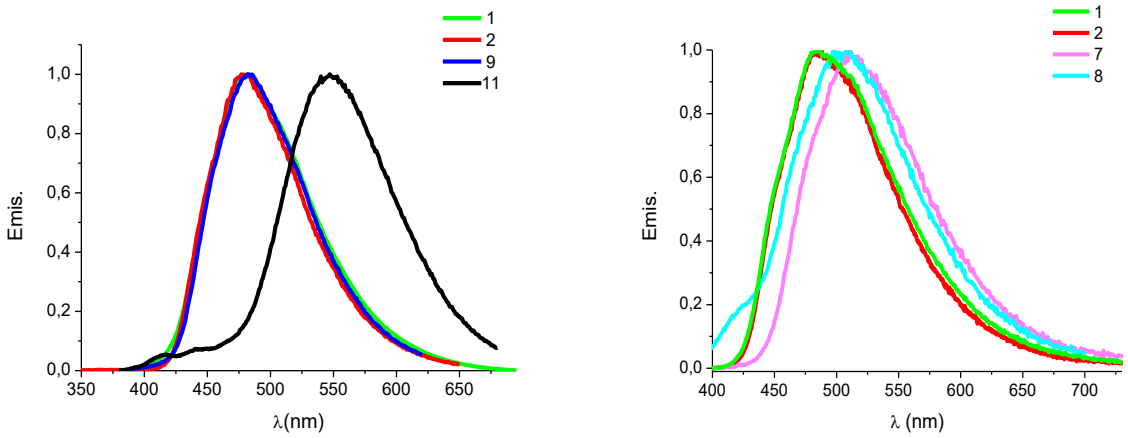

Fig. 4. a: Normalized fluorescence spectra of compounds **1**, **2**, **9** and **11** in dichloromethane; b: fluorescence spectra of compounds **1**, **2**, **7** and **8** in dichloromethane.

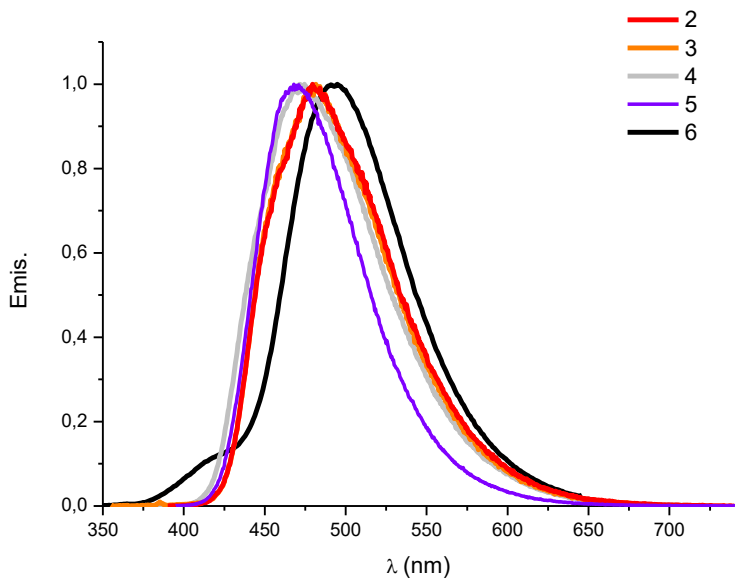

Fig. 5. Fluorescence spectra of compounds **2-6** in dichloromethane.

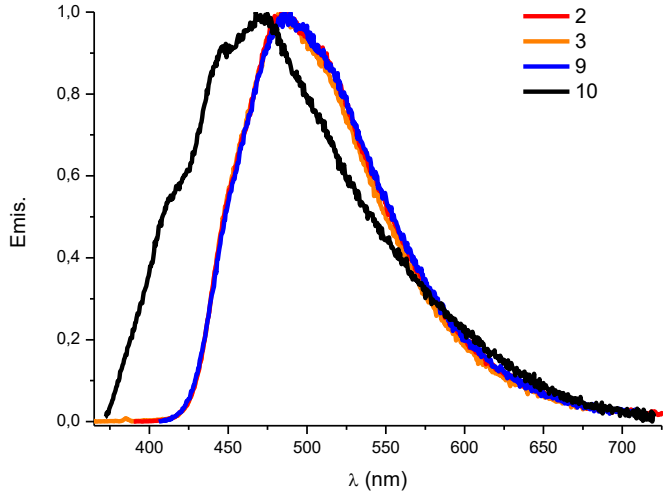

Fig. 6. Fluorescence spectra of compounds **2**, **3**, **9** and **10** in dichloromethane.

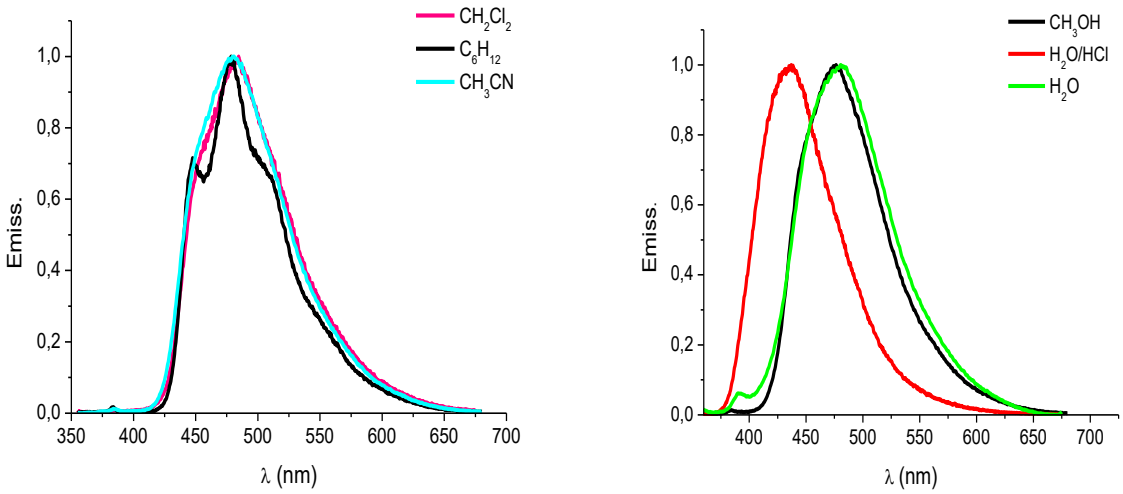

Fig. 7. Emission spectra in different solvents.

Table **4**. Absorption spectroscopic data in different solvents.						
	Cicloesane λ_{abs} (nm)	CH_2Cl_2 λ_{abs} (nm)	CH_3CN λ_{abs} (nm)	CH_3OH λ_{abs} (nm)	H_2O λ_{abs} (nm)	H_2O/HCl 1M λ_{abs} (nm)
1	299 374	306 367	295 364	295 354	270 338	270 330
2	302	306 342sh 385sh	305	301	305	329
3	310 340	316 345	304 343	299	299	290 324

4	303	305 374sh	300	298	291 330	
5	299 377	301 380	301 377	296 372	305 430	283 352
6	315	316 372	317 345	315	300 341	284 338
7	300 382	308 380	309 381	300 372	314 390	285 360
8	305 352	305 353	304 350	300 348	314 360	293 362
9	293 362	305 358	293 355	291 350	297 328 367	288 336
10	361	314 362	355	343	280 355	279 338
11	375	304 366 380	375	366	375	358 373 394

Table **5**. Fluorescence emission data in different solvents.

	Cicloesane λ_{abs} (nm)	CH_2Cl_2 λ_{abs} (nm)	CH_3CN λ_{abs} (nm)	CH_3OH λ_{abs} (nm)	H_2O λ_{abs} (nm)	H_2O/HCl 1M λ_{abs} (nm)
1	475	485	467	473	470	440
2	445 476 508	484	478	477	479	433
3	479	484	480	474	481	437
4	477	479	481	475	481	435
5	444 472 500	477	453	487	470	459
6	482	495	509	500	512	430
7	482	506	506	500	507	472
8	462 490 522	491	492	488	498	516
9	478	486	480	475	475	440
10	407 436 465	467	435	433	440	437

11	500	548	577	552	530	480

a)

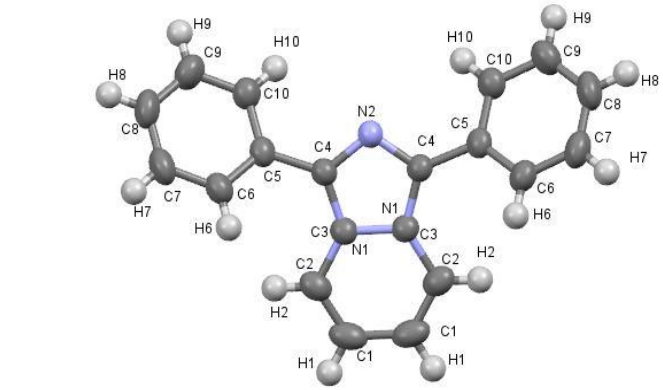

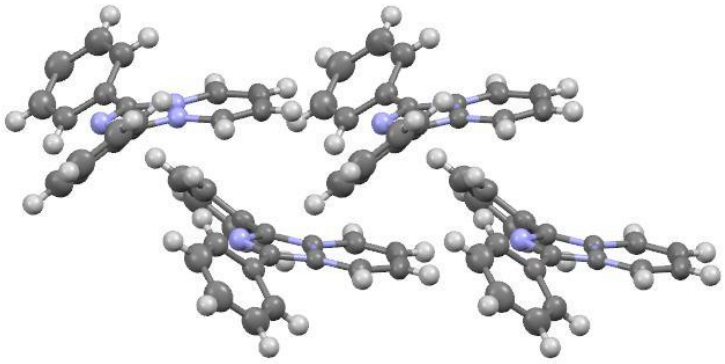

b)

Fig. 8. Molecular structure (a) and packing in the crystal structure (b) of compound **2**.

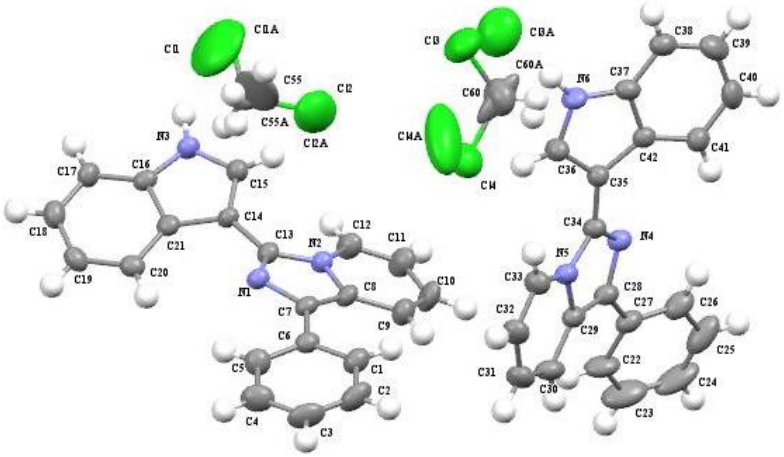

a)

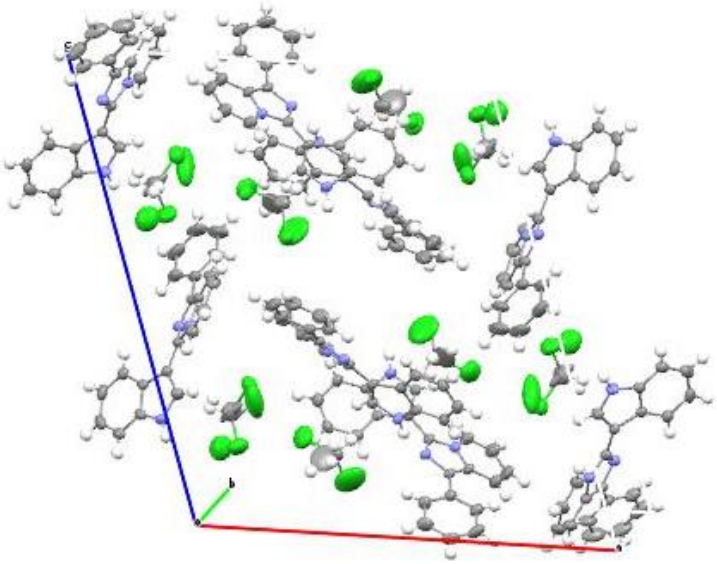

b)

Fig. 9. Molecular structure (a) and packing in the crystal structure (b) of compound **7**.

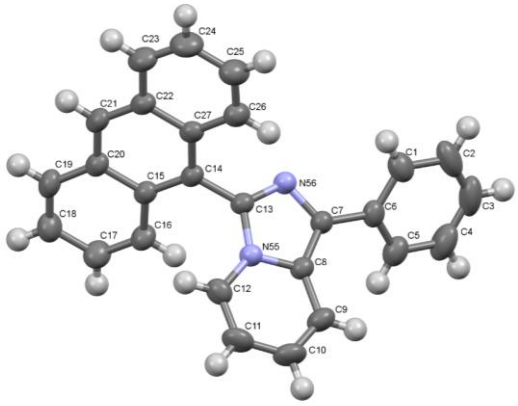

a)

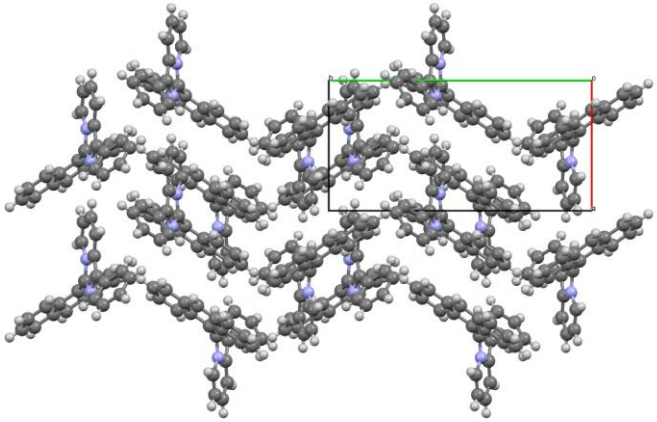

b)

Fig. 10. Molecular structure (a) and packing in the crystal structure (b) of compound **11**.

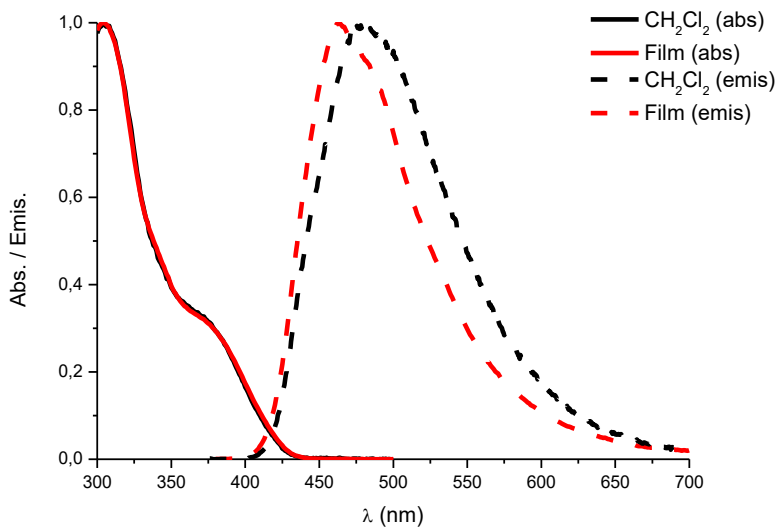

Fig. 11. Absorption and emission spectra of compound **4** in the polyurethane film and in dichloromethane.

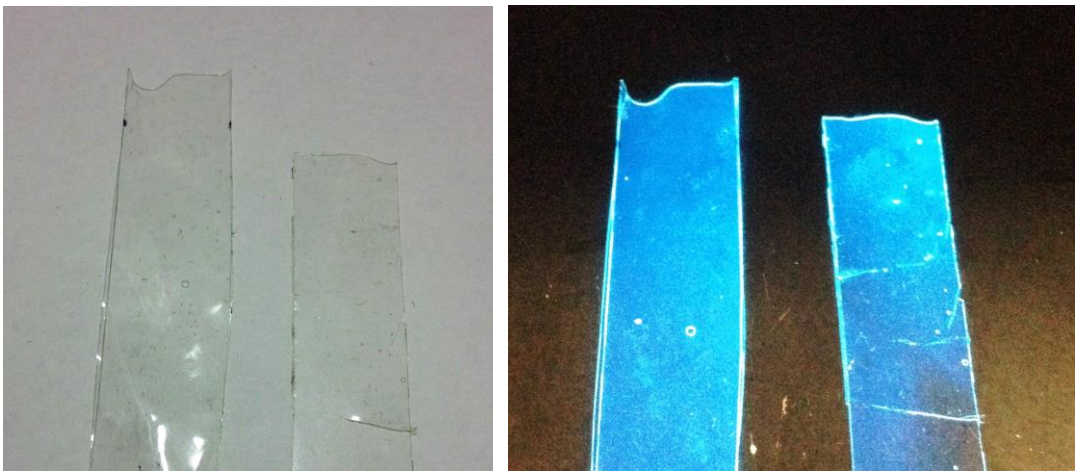

Fig. 12. Polyurethane film with compound **4** under normal lighting (left) and UV lamp (right).